



## Structural Properties of the Nanocrystallized Magnetite of Different Syntheses

V.N. Kuznetsov<sup>1,\*</sup>, A.S. Stanislavov<sup>1,†</sup>, S.N. Danilchenko<sup>1</sup>, O.V. Kalinkevich<sup>1</sup>, A.N. Kalinkevich<sup>1</sup>,  
L.F. Sukhodub<sup>2</sup>

<sup>1</sup> Institute of Applied Physics, 58, Petropavlovskaya Str., 40000 Sumy, Ukraine

<sup>2</sup> Sumy State University, 2, Rymsky Korsakov Str., 40007 Sumy, Ukraine

(Received 9 June 2013; revised manuscript received 1 July 2013; published online 31 August 2013)

Transmission electron microscopy (TEM) with electronic diffraction and X-ray diffraction (XRD) was used to study structural features of nanosized magnetite  $\text{Fe}_3\text{O}_4$ , which was synthesized using polymeric matrices (polysaccharide chitosan, at alias). From the received data it was revealed that growth inhibition and size stabilization of  $\text{Fe}_3\text{O}_4$  nanoparticles were strongly affected by polysaccharide matrix. It was also observed that directional size decrease of  $\text{Fe}_3\text{O}_4$  nanoparticles was accompanied by the increasing defectiveness of crystal lattice and decreasing unit cell size. The effectiveness of complementary use of both TEM with electronic diffraction and XRD techniques for structural and substructural parameters determination while studying magnetite nanosized particles synthesized in polysaccharide matrices is shown in this paper.

**Keywords:** Magnetic nanoparticles, Biopolymer matrix, Chitosan, XRD, TEM, Particles size.

PACS numbers: 61.72. – y, 75.50.Tt

### 1. INTRODUCTION

Nowadays materials based on nanosized magnetite  $\text{Fe}_3\text{O}_4$  particles are widely used in the modern medicine and technics [1]. The key question in the development of methods of the materials creation is the nanoparticles size control since all application fields of nanomaterials based on  $\text{Fe}_3\text{O}_4$  are supported by the strict dependences of its service properties from the particles sizes and their monodispersion.

The known methods of the magnetite nanoparticles stabilization are, for example: the creation of the oriented layers of the polarized organic molecules on its surface [1], the use of the biomolecules chelating effect [2] or the synthesis in the biopolymer matrix [3]. The polysaccharides and, especially, chitosan (Ch) are utilized as effective stabilizing agents for magnetite nanoparticles [2]. Chitosan and its derivatives are widely used in the creation of different biomedical materials due to their remarkable biological and chemical properties [4]. The presence of  $\text{OH}^-$  and  $\text{NH}_2$  radicals allows to assume the possibility of triggering the growth inhibition mechanism of the magnetite nanoparticles in the presence of chitosan macromolecules.

### 2. MATERIALS AND METHODS

#### 2.1 Materials

The “Mgn 1” sample was synthesized using the classic thermochemical method and was used for comparison as a sample with relatively high crystallite particles sizes. The synthetic magnetite was received by the deposition in the alkaline medium (5 % NaOH) from the bivalent and trivalent iron salt solution  $(\text{NH}_4)_2\text{SO}_4 \cdot \text{FeSO}_4 \cdot 6\text{H}_2\text{O}$  and  $\text{FeCl}_3 \cdot 6\text{H}_2\text{O}$ , salt molar ratio 2,41:1 for 2 minutes at 100°C for “Mgn 2” and at 80°C for “Mgn 3”. The derived powder was washed by

the decantation and dried. During the decantation “Mgn 3” was affected by the static magnetic field.

Magnetite samples inside the biopolymer matrix were derived adding the bivalent and trivalent iron salt solutions into the 0,5% lowmolecular chitosan solution in the 1% acetic acid (salt molar ratio 2,41:1, chitosan to magnetite ratio 50:50). The codeposition was made by: (1) the addition of the mother liquor into the boiling NaOH (ChMgn 1), (2) the addition of the 5% NaOH to the mother liquor at 80°C (ChMgn 2) or (3) the 10%  $\text{NH}_3$  solution at the room temperature (ChMgn 3). The samples were washed by the decantation and dried.

#### 2.2 Methods

The crystallinity and structure of the synthesized samples were examined using an X-ray diffractometer DRON-4-07 (Bourestnik, Inc., Saint-Petersburg, Russian Federation) connected to a computer-aided system for the experiment control and data processing. The Ni-filtered  $\text{CuK}\alpha$  radiation (wavelength 0,154 nm) with a conventional Bragg–Brentano  $\theta$ -2 $\theta$  geometry was used. The current and the voltage of the X-ray tube were 20 mA and 40 kV respectively. All experimental data was processed by means of the program package DIFWIN-1 (Etalon PTC, Ltd., Moscow, Russian Federation). Identification of crystal phases was done using a JCPDS card catalog (Joint Committee on Powder Diffraction Standards).

The crystallite sizes  $L$  were calculated using the Scherrer equation and by the three-fold convolution method considering the influence of small sizes of coherent scattering regions and deviations of interplanar spaces between a sample and a standard in which microstrains are absent  $\varepsilon$  using the best approximation function (Gauss or Cauchy) for each contribution characterization on the peak broadening [5].

\* [vkuznetsov.ua@gmail.com](mailto:vkuznetsov.ua@gmail.com)

† [tornado200@yandex.ru](mailto:tornado200@yandex.ru)

The extrapolation function method was used for the crystal lattice parameter calculation. This method allows to extrapolate the lattice parameter value to the  $2\theta = 90^\circ$  where the interplanar spaces' definition error as well as the lattice parameter's one is extremely low. The Nelson-Riley extrapolation function was used in our studies [6].

Electron microscopic and electron diffraction studies were conducted after the samples ultrasonic dispersion using the transmission electronic microscope PEM-125K (SEMI, PTC, Sumy, Ukraine) with the 90 kV accelerating voltage and the 100  $\mu$ A beam current. The aperture diaphragm width was 0,1 mm in the electron diffraction mode, the intermediate lenses worked without the magnification. The measurement of the magnetite linear crystallite particle sizes was performed using the VideoTesT-Razmer 5.0 program (VideoTesT, Ltd., Saint-Petersburg, Russian Federation).

### 3. RESULTS AND DISCUSSION

The X-Ray phase analysis showed that the all studied samples consist of the  $\text{Fe}_3\text{O}_4$  magnetite (JCPDS 19-629) phase with the different degree of crystallinity (Fig. 1). In  $\text{Ch}/\text{Fe}_3\text{O}_4$  composites the crystallite sizes are significantly smaller compared to the  $\text{Fe}_3\text{O}_4$ , synthesized without the polysaccharide matrix.

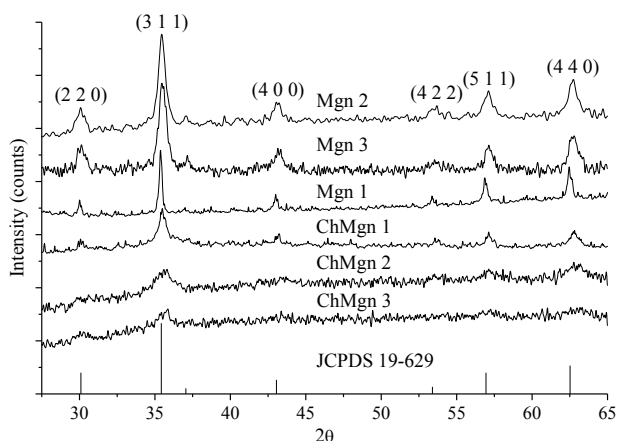


**Fig. 1** – XRD spectra of magnetite samples and chitosan/magnetite composites

The results of the structural and substructural characteristics calculations according to the X-Ray diffraction (XRD) are shown in Table 1. The decrease of the crystallite sizes in case of the synthesis with the polysaccharide matrix is conducted by the decrease of the unit cell size. The differences in crystallite size values calculated using the Scherrer equation for (2 2 0) and (4 4 0) peaks could be explained with by the significant contribution of the lattice microstrain to the peak physical broadening. The ab-

solute values of the lattice microstrains are sufficiently great (0,005 – 0,018) and show the expressed uptrend with the decrease of the crystallite sizes.

**Table 1** – Structural and substructural characteristics of magnetite samples according to the XRD

Sample	Unit Cell Parameters by Nelson-Riley, nm	Crystallite Sizes by Scherrer, nm	Three-Fold Convolution	
			$L$	$\langle \varepsilon^2 \rangle^{0,5} \cdot 10^{-3}$
Mgn 1	0,84013	37,3 (2 2 0) 46,7 (4 4 0)	33,9	0,8
Mgn 2	0,83767	14,6 (2 2 0) 22,2 (4 4 0)	13,4	2,7
Mgn 3	0,83688	10,7 (2 2 0) 14,2 (4 4 0)	9,9	3,3
ChMgn 1	0,83457	4,1 (2 2 0) 7,9 (4 4 0)	3,8	9,8
ChMgn 2	0,83779	7,0 (2 2 0) 5,3 (4 4 0)	8,3	8,7
ChMgn 3	0,83553	5,1 (2 2 0) 7,4 (4 4 0)	4,8	7,4

The micrographs of the nanoparticle clusters with the different magnification and microdiffraction patterns were obtained by the TEM (e.g., Fig. 2). The comparative analysis of the electron microscopy data validates very well with the XRD data showing the decrease in the sizes of the crystalline particles synthesized in the presence of the polysaccharide matrix.

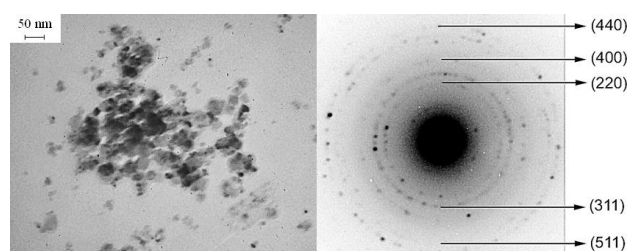


**Fig. 2** – The micrograph and the microdiffraction pattern of the “Mgn 3” sample

### 4. CONCLUSIONS

The magnetite deposition in the biopolymer matrix significantly decreases the sizes of the derived  $\text{Fe}_3\text{O}_4$  nanoparticles which indicate that chitosan inhibits the processes of the  $\text{Fe}_3\text{O}_4$  creation and growth. The directed decrease of the  $\text{Fe}_3\text{O}_4$  nanoparticles by the inclusion of the biopolymer growth inhibitors, alkali, ammonia, synthesis temperature raising is followed by the increase of the nanoparticles crystal structure imperfection and the decrease of their unit cell sizes.

### REFERENCES

1. P. Berger, N.B. Adelman, K.J. Beckman, D.J. Campbell, A.B. Ellis, G.C. Lisensky, *J. Chem. Educ.* **76**, 943 (1999).
2. Y. Wang, B. Li, Y. Zhou, Yu Zhou, D. Jia, *Nanoscale Res. Lett.* **4**, 1041 (2009).
3. J. Giri, S.G. Thakurta, J. Bellare, A.K. Nigam, D. Bahadur, *J. Magn. Mater.* **293**, 62 (2005).
4. M. Rinaudo, *Prog. Polym. Sci.* **31**, 603 (2006).
5. A.S. Cagan, L.M. Shishlyannikova, A.P. Unikel, *Fact. Lab.* **46**, 903 (1980).
6. H.P. Klug, L.E. Alexander, *X-Ray Diffraction Procedures: For Polycrystalline and Amorphous Materials* (New York: Wiley: 1974).